Remarkable photocatalytic performance of zinc oxide nanoparticles prepared through green synthetic method by using *Citrus limon* dry peel extract

Sushan Waiba[*], Motee Lal Sharma[**] and Kamal Prasad Sapkota[**]

[*]Department of Chemistry, Amrit Campus, Tribhuvan University, Kathmandu, Nepal.

[**]Central Department of Chemistry, Tribhuvan University, Kirtipur, Kathmandu, Nepal.

Abstract: Zinc oxide nanoparticles (ZnO NPs) were synthesized through green synthetic method using *Citrus limon* (Lemon) dry peel extract which acts as a reducing agent. The synthesized nanoparticles were yellowish white and their UV-vis spectra showed the characteristic maximum peak at 332 nm which affirmed the formation of zinc oxide nanoparticles. For further confirmation, the synthesized nanoparticles were characterized through X-ray Diffraction (XRD), Fourier Transform Infrared Spectroscopy (FT-IR), Field Emission Scanning Electron Microscopy (FE-SEM) and High-Resolution Transmission Electron Microscopy (HR-TEM). The most intense peak in the XRD pattern was selected for crystallite size determination by using the Scherrer's equation; the average crystallite size was computed to be 19 nm. FE-SEM results demonstrated the spherical shape of nanoparticles with less distinct morphology. The hexagonal structure of ZnO NPs was identified by HR-TEM. ZnO NPs showed excellent catalytic activity of 50.25% photodegradation of MB under natural sunlight irradiation for 120 minutes. The results show that the as-synthesized ZnO NPs can have possible application in water treatment for removing harmful dyes. The phytochemical screening of dry *Citrus limon* peel extract revealed the presence of alkaloids, flavonoids, cardiac glycosides, saponins, terpenoids, tannins, and reducing sugar.

Keywords: *Citrus limon* peel extract; Green synthesis; Photodegradation; Reducing agents; Zinc oxide nanoparticles.

Introduction

Nanotechnology is an emerging field that specializes in the production of nanomaterials. The rise of nanoscience has given a new interdisciplinary field all over the world, and people appreciate science at the nanoscale[1]. Nanoscience and nanotechnology are the branches of science that deal with the production and characterization of 1-100 nm at least one dimension in size and inspection at the molecular level. Metal and metal oxide nanoparticles have various applications in physics, chemistry, biology, engineering and materials science[2-7]. The consolidation of nanoscience and biology has attracted many researchers. Initially, the focus was on the biosynthesis of Ag and Au nanoparticles, but currently, the green synthesis of metal oxide nanoparticles is at the forefront [3,8-10]. Biological compounds present in plants act as capping agents in the synthesis of nanoparticles, which play a versatile role in stabilizing them[4].The importance of nano-size materials over bulk phase is because of their eminent physical, chemical, and biological properties, and the atoms present on the surface tend to be more active than those of the center. These unique properties make nanoparticles more superior than bulk ones. For the production of nanoparticles on a large scale, the biosynthesis of nanoparticles using plants is very superior. The nanoparticles produced from plants are of various shapes and sizes as compared with those produced from other organisms such as bacteria, fungi and algae[5-16]. Because of their extremely small size and large surface area, metal and metal oxide nanoparticles have been found to be promising in the field of nanotechnology. Metal oxide nan-

Author for Correspondence: Kamal Prasad Sapkota, Central Department of Chemistry, Tribhuvan University, Kirtipur, Kathmandu, Nepal.
Email: mychemistry2037@gmail.com / kamal.sapkota@cdc.tu.edu.np; https://orcid.org/0000-0002-0452-7796

Received: 19 Mar, 2024; Received in revised form: 23 Apr, 2024; Accepted: 01 May 2024.
Doi: https://Doi.org/10.3126/sw.v17i17.66450

oparticles are known for their captivating properties like antimicrobial, magnetic and catalytic[17-24].

The nanoparticles in the nanoscale range show promising antimicrobial activities. The antibacterial activities depend on the size of nanoparticles. Their size is important because they can penetrate through cell wall[7].

There are various processes used in the synthesis of zinc oxide nanoparticles, such as physical and chemical methods[25-30]. These techniques use chemicals as stabilizing agents, which are costly. In the present work, nanoparticles have been synthesized using eco-friendly materials that act as reducing and capping agents. Citrus fruits are known to be rich in vitamins and minerals, but their peels are usually discarded. Citrus peels consist of γ-terpinene, terpinolene, d-limonene and citral, which are beneficial to health if utilized in a proper way.

The literature presents numerous reports on the green synthesis of nanoparticles using fruit extracts. However, only a few researchers have focused on the synthesis of ZnO NPs using *Citrus limon* (lemon) peel extracts. Furthermore, the available literature for the synthesis of ZnO NPs using *Citrus limon* peel extract and their photocatalytic application is not sufficient. Hence, the current research work focuses on the green synthesis of ZnO NPs using dry *Citrus limon* peel extract and their application in the photocatalytic degradation of methylene blue under natural sunlight irradiation.

Materials and methods

Chemicals

Zinc Nitrate Hexahydrate (96-100% Fischer scientific), Sodium hydroxide pellets (97% LOBA CHEMIE PVT LTD), Methylene blue (70%, fine-chem limited) and Ethanol were used as purchased. Distilled water was employed to prepare all solutions.

Instruments

Digital Weighing Balance, Hot air oven, Magnetic stirrer (LABINCO L34), Centrifuge (REMIRU), Sonicator, Auto deluxe digital pH meter, Dryer, X-Ray Diffraction, UV-Visible spectrophotometer (Labtronics Model LT -2802), Field Emission Scanning Electron Microscopy (FE-SEM, SUB 8230, Hitachi, Chiyoda-ku, Tokyo, Japan), Transmission Electron Microscopy (HR-TEM, JEM-2200FS, JEOL, Akishima, Tokyo, Japan), and Fourier Transform Infrared Spectroscopy (FTIR, TRACER-100) were employed as major instruments.

Method

Phytochemical screening

Waste peels of lemon were collected, dried and crushed into powder. 10 grams of peel powdered in 100 mL of was heated in water bath at 80 °C for 30 min and left for 24 hours. Then, the aqueous extract was filtered and phytochemical tests were performed.

Firstly, the lemon was washed with tap water, and the peel was separated from the fruit. The peel was washed with double-distilled water to remove external impurities present on the peel and left in shadow for 10 days to dry up. Dry peel was crushed in a mixture grinder to obtain its powder form. About 50 grams of powdered peel were taken in a 500-mL beaker containing 300 mL of distilled water and then boiled at 80 °C for 20 minutes and filtered through Whatman 41 filter paper to remove insoluble impurities. The resultant filtrate was stored at 4 °C.

Synthesis of zinc oxide nanoparticles

In the synthesis of zinc oxide nanoparticles, lemon peel extract was used as a reducing agent. Three different concentrations of solution were prepared. Initially, 8 g, 10 g, and 12 g of zinc nitrate hexahydrate were dissolved in 100 mL of deionized water using a magnetic stirrer for 10 minutes. Then, 30 mL of freshly prepared lemon peel extract were added. After 5 minutes, the pH of the solution was maintained at 9 with a dropwise addition of NaOH. The mixture was continuously stirred on a magnetic stirrer at 70 degrees Celsius for 30 minutes. The yellowish-white precipitate was observed, which was collected by centrifugation at 4000 RPM and washed with ethanol for further purification. The prepared ZnO nanoparticles were

dried in an oven at 80 °C for 8 hours and stored in an airtight vial.

Photocatalytic degradation of methylene blue

The photodegradation of methylene blue was detected in the presence of ZnO NPs under sunlight exposure, and the decrease in absorbance was determined by using a UV-Vis spectrophotometer. In an aqueous solution of methylene blue (10 ppm), photocatalysts prepared from three different concentrations (0.27, 0.3, and 0.4 M of precursor) of mass 0.012 g were added separately, and photodegradation was studied under sunlight. At regular intervals of time, the reaction was observed spectrophotometrically at room temperature. Reaction mixtures' color started to fade, revealing that degradation had started.

Results and Discussion

Phytochemical screening of lemon peel extract

The term 'phyto' is derived from the Greek word which means plant. The naturally occurring chemical substances present in plants are called phytochemicals. The phytochemicals have either favourable or unfavourable effects on human health. The phytochemical ingredients in a plant determine its medicinal values. Previously, plants were utilized directly but currently active ingredients have been detected and extracted in their purest form. Different solvents used for the extraction process are ethanol, water, benzene and methanol. The detection of phytochemicals in plants assists in the prediction of any plants in the application of pharmacology[27].

The phytochemical screening is observed in aqueous extract. Various phytochemicals present in the aqueous extract were alkaloid, flavonoid, cardiac glycosides, saponins, terpenoid, tannins and reducing sugar.

UV-visible absorption spectra of ZnO NPs

UV-vis spectroscopy serves as one of the best methods for characterizing nanoparticles. UV-vis spectra of lemon peel extract showed a strong peak at 331 nm at pH = 9.

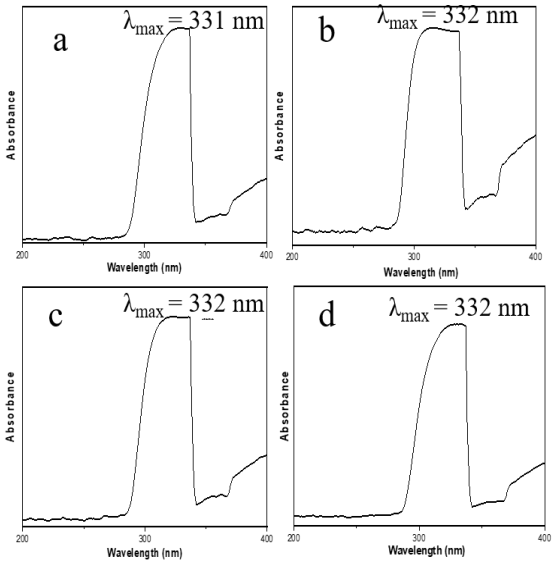

Figure 1: UV-vis absorption spectrum: (a) Lemon peel extract (b) 0.27M ZnO NPs (c) 0.30M ZnO NPs (d) 0.40M ZnO NPs.

The result is entirely according to those of Mehta *et al.* (2019) in which Ag NPs were synthesized using orange peel extract. The UV-Vis absorption of all three concentration of ZnO also shows the strong sharp peak at 332 nm.

Fourier transform infrared (FTIR) spectroscopy

The possible functional groups contained in the lemon peel extract that behaved as the effective reducing agent were identified using FT-IR spectroscopy and the corresponding information is presented in Figure 2.

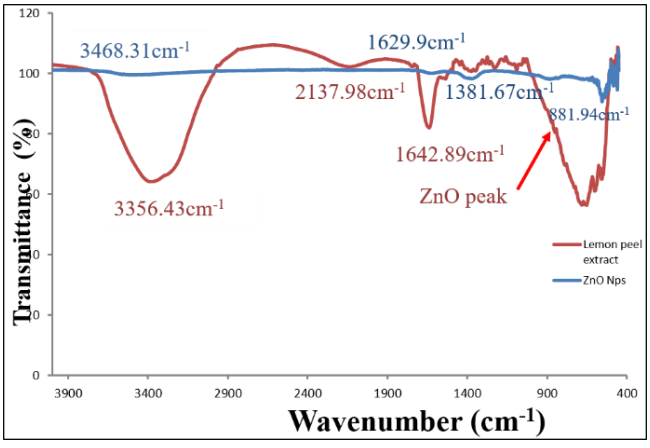

Figure 2: FTIR spectra of lemon peel extract and ZnO NPs prepared from 0.4M concentration of precursor.

Distinguishing peaks at 3468.31 and 3356.43 cm^{-1} can be attributed to the hydrogen bonded O-H groups of alcohols

or phenols and N-H groups of amides. Similarly, the maxima at 1629.9 and 1642 cm^{-1} are attributed to O-H stretching or chlorophyll found in plants[18]. The peak at 2137.98 cm^{-1} corresponds to C-H stretching[25]. Lemon peels mainly contain alkaloids, flavonoids, cardiac glycosides, saponins, terpenoids, tannin, and reducing sugar[23,24]. The FTIR spectrum of the ZnO NPs (Figure 2, blue curve) demonstrates that most of the functional groups present in the peel extract were retained in the as-synthesized nanoparticles. Less intense peaks seen in the spectrum of ZnO NPs compared to those in extract are assigned to the very low concentration of those molecules.

X-ray diffraction (XRD) analysis

The primary purpose of XRD is to investigate the phase geometry of synthesized nanoparticles. The crystallinity and crystalline nature of the prepared ZnO NPs was assured via X-ray diffractometric analysis and corresponding profiles are presented in Figure 3. The XRD profiles display characteristic peaks at 2θ values of 31.75, 34.40, 36.16, 47.51, 56.52, 62.70, 66.24 and 68.90 degrees, which correspond to 100, 002,001, 102, 110, 103, 200, 112 and 201 crystal planes of the hexagonal wurtzite ZnO, respectively. The characteristic diffraction peaks with related crystal planes of hexagonal wurtzite geometry of ZnO NPs has been well supported with the results reported in the literature (JCPDS-36-1451)[30]. The crystallite size of the prepared nanoparticles was calculated using the Scherrer's formula; the 2θ position of the most intense diffraction peak was selected to determine the crystallite size of the ZnO NPs. The Scherrer's equation is presented in equation (x).

$$D = K\lambda/\beta \cos\theta \quad \ldots\ldots\ldots\ldots\ldots\ldots\ldots\ldots \text{(x)}$$

Where, D is size of crystallites, K is Scherrer's constant = 0.94, λ is X-ray wavelength = 0.14518 nm, β is FWHM (Full Width at Half Maximum) in radian (β = 0.47078, determined from the most intense peak), Bragg's angle 2θ (intense peak position) = 36.16°. Using equation (x) and all these values, the size of crystallites was found to be 18.55 ≈ 19 nm.

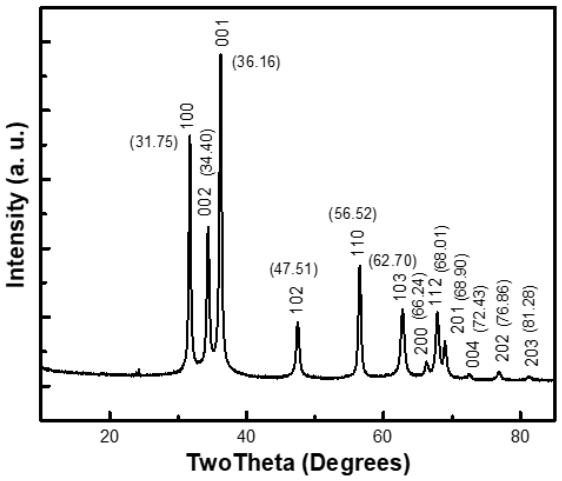

Figure 3: XRD pattern of ZnO NPs synthesized from 0.4 M concentration of precursor using lemon peel extract.

The characteristic diffraction peaks with prominent intensity assure that the as-synthesized ZnO NPs possess crystalline form. The crystalline nature of the nanoparticles is responsible for notable applications in diverse fields.

Field emission scanning electron microscopy (FE-SEM)

The shape and size (i.e., morphological features) of photocatalysts are one of the crucial factors that affects photocatalytic efficiency. Hence, FE-SEM analysis was employed used to determine the surface morphology of the synthesized nanoparticles.

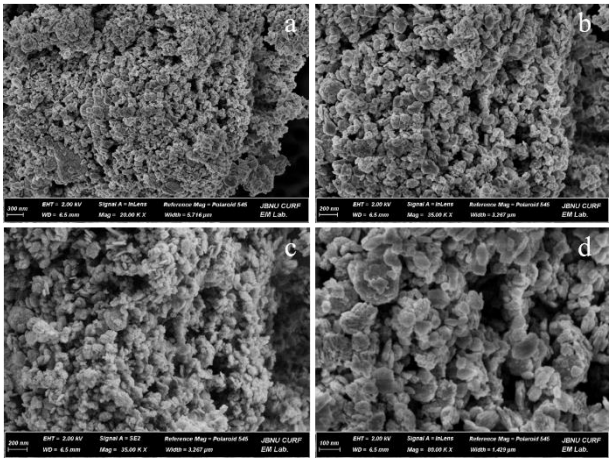

Figure 4: FE-SEM images of the as-synthesized ZnO NPs.

According to FE-SEM images, the ZnO nanoparticles are seen in the form of discrete clusters. The particles are seen more aggregated leading to less distinct shapes. The FE-

SEM findings are in good agreement with those reported in the literature[29].

High-resolution transmission electron microscopy (HR-TEM)

Fine morphology and microstructure of the as-prepared nanoparticles were analyzed through high-resolution transmission electron microscopy (HR-TEM) and the corresponding images are presented in Figure 5. Relatively lower resolution images reveal that the as-synthesized ZnO NPs in are seen in the form of aggregates of particles. The nanoparticles are mostly irregular with some particles having the shape of coarse rice grains, which are linked with one another forming discrete clusters.

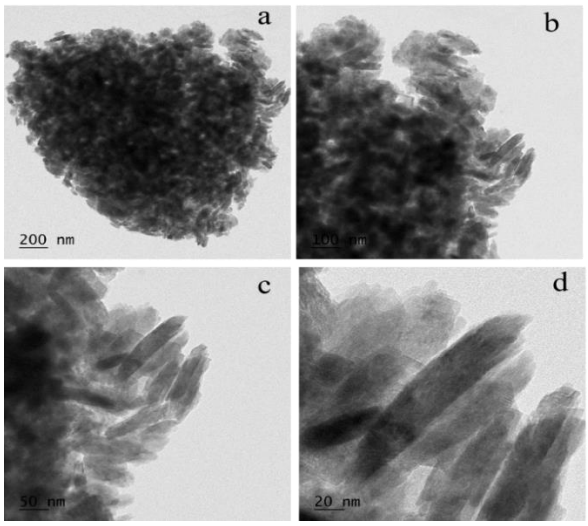

Figure 5: HR-TEM images of ZnO NPs; (a) and (b) lower resolution and (c) and (d) higher resolution.

Higher resolution images display the smaller nanoparticles in close association with other nanoparticles. The nanoparticles are seen with differing sizes ranging from 20 nm to 200 nm. The findings of HR-TEM analysis are consistent with those of reported in the literature[6].

Photocatalytic degradation of methylene blue

Photocatalysis is becoming a more common option for the degradation of organic contaminants as compared to other methods; photocatalysis has many benefits, such as complete mineralization, which prevents problems with subsequent recycling of wastes, and cheap operating costs. The photocatalytic execution of three different concentrations of ZnO NPs was examined by same method at similar condition. The UV-vis range was set between 200 to 800 nm for the spectra matching to photodegradation of MB.

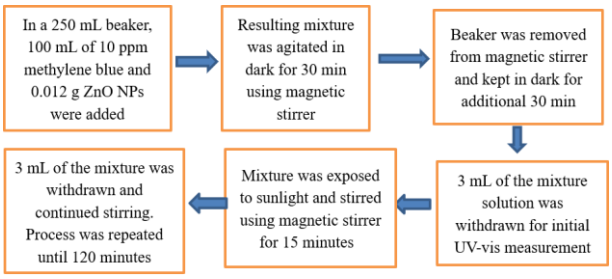

Scheme 1: Flowsheet representation of the process of photocatalytic degradation of MB.

In photocatalytic reaction, three different samples of mass 0.012 g were tested on 10 ppm methylene blue solution using natural sunlight irradiation.

Table 1: Concentration of zinc nitrate hexahydrate (precursor) for nanoparticles synthesis and labelling of different samples.

Sample	Conc. of $Zn(NO_3)_2.6H_2O$	Plant extract
ZnO-A	0.27 M	30 mL
ZnO-B	0.30 M	30 mL
ZnO-C	0.40 M	30 mL

Figure 6 illustrates that the sample designated as ZnO-C revealed best photocatalytic potential among all three samples, i.e., it resulted in 50.25% photodegradation of MB solution within 2 hours of solar irradiation. The results are supported by the findings of Sapkota *et al*. (2020) which reported 54.2% photodegradation of MB using pristine CuO[26]. In the photocatalytic experiments, sample ZnO-A and sample ZnO-B revealed photodegradation of 35.18% and 48.69%, respectively. Since the ZnO-C sampled displayed the best photocatalytic performance, this sample was chosen for the further experiments. The best

photocatalytic performance of the ZnO-C sample may be attributed to the optimum concentration of precursor (zinc nitrate hexahydrate) solution for the complete conversion of the precursor into effective ZnO photocatalyst.

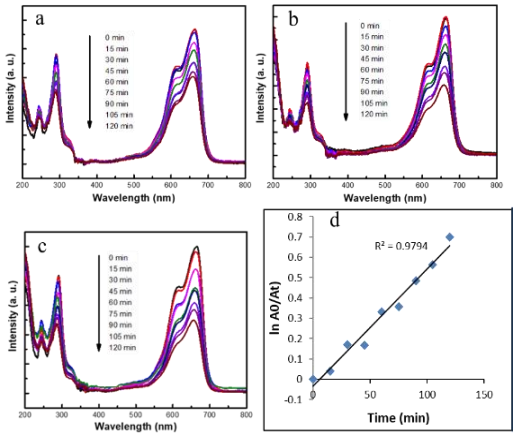

Figure 6: Photodegradation of MB: (a) ZnO-A (b) ZnO-B (c) ZnO-C nanoparticles for 120 min of sunlight exposure with interval time of 15 min, (d) Degradation kinetics of MB by the catalytic action of ZnO NPs.

The photodegradation of MB by the ZnO NPs photocatalyst was found to follow the pseudo first order kinetic model. The deterioration rate constant can be calculated by following equation.

$$\text{Ln } C_o/C_t = Kt \quad \ldots\ldots\ldots\ldots\ldots\ldots \text{(iii)}$$

Where C_o = Initial concentration, C_t = Concentration at time "t", K = Rate constant and t = Time interval of irradiation (min).

The deterioration rate constants during the photodegradation of MB by the action of ZnO-A, ZnO-B and ZnO-C were computed to be 0.006711, 0.05644 and 0.05759, respectively.

Based on the data obtained from characterization and photocatalytic experiments and those available in the literature, the alternative mechanism of photocatalytic action has been proposed.

The electron in the filled valence band (VB) of ZnO photocatalyst with MB solution get excited and move to conduction band (CB) when photocatalyst is subjected to solar-irradiation with the energy corresponding to or exceeding its band gap energy.

$$ZnO + h\nu \longrightarrow e^-_{CB} + h^+_{VB} \quad \ldots\ldots\ldots \text{(iv)}$$

$$e^-_{CB} + h\nu \longrightarrow \text{Energy} \quad \ldots\ldots\ldots\ldots\ldots\ldots\ldots\ldots\ldots \text{(v)}$$

The electrons on CB reduce the dissolved oxygen (O_2) to superoxide radicals ($O_2^{\cdot-}$), which is quickly reduced to the potent oxidant, namely hydroxyl radicals (·OH). Methylene blue molecules that are present near the surface of photocatalyst are broken down by these hydroxyl radicals.

$$e^-_{CB} + O_2 \longrightarrow O_2^{\cdot-} \quad \ldots\ldots\ldots\ldots\ldots\ldots \text{(vi)}$$

The H^+ and hydroxyl radicals ($OH^{\cdot}$) are created when the holes react with water molecules.

$$h^+_{VB} + H_2O \longrightarrow H^+ + OH^{\cdot} \quad \ldots\ldots\ldots\ldots\ldots \text{(vii)}$$

The superoxide ($O_2^{\cdot-}$) and $OH^{\cdot}$ reacts with pollutants to produce H_2O and CO_2.

$$O_2^{\cdot-} + MB \longrightarrow H_2O + CO_2 \quad \ldots\ldots\ldots \text{(viii)}$$

$$OH^{\cdot} + MB \longrightarrow H_2O + CO_2 \quad \ldots\ldots\ldots \text{(ix)}$$

The mechanism of photocatalytic decomposition of MB by the action of ZnO NPs has been demonstrated in Figure 7(a).

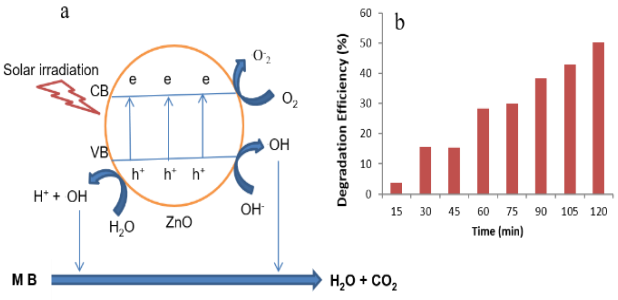

Figure 7: (a) Mechanism of Photodegradation of MB by ZnO NPs and (b) Graphical representation of degradation of MB at different interval of time.

The optimum dose (mass) of the best photocatalyst sample (ZnO-C) was determined by using different doses of the photocatalyst to photodegrade the same volume of MB with same concentration under the similar experimental conditions. Among the different doses tested (0.0092 g,

0.012 g and 0.032 g of the ZnO-C photocatalyst), 0.012 g dose of the photocatalyst displayed the best photocatalytic performance. The photodecomposition trends of MB by 0.0092 and 0.032 g of ZnO-C photocatalyst sample are presented in Figure 8 (a) and (b).

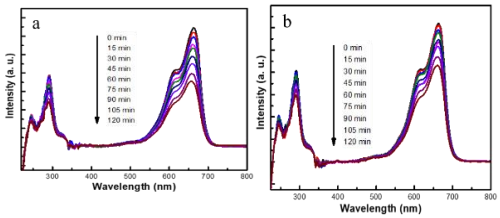

Figure 8: (a) Photodegradation observed as mass of the photocatalyst was increased to 0.032 g and (b) Photodegradation observed as the mass of photocatalyst was decreased to 0.0092 g.

Initially, 0.012 g of photocatalyst dose was taken arbitrarily for the photocatalytic experiments. Hence, other doses of the photocatalyst were also tested to identify the optimum dose of the photocatalyst. When the mass of photocatalyst was increased to 0.032 g, the deterioration of MB solution observed was 43%, which showed a remarkable decrease in performance compared to that of 0.012 g dose. Similar effect was observed as the dose of the photocatalyst was decreased. When the mass of photocatalyst was decreased to 0.0092 g, the deterioration of MB observed was 30.08%, displaying a sharp decrease in the photocatalytic performance. Therefore, 0.012 g dose of the photocatalyst was used as the optimum mass (dose) in all photocatalytic experiments. The greater photocatalytic activity of 0.012 g dose of photocatalyst is attributed to the optimum dose because the optimum dose supplies the required number of active sites on the photocatalyst surface. The larger number of active sites will produce the larger proportions of reactive oxygen species to decompose MB solution. However, the photodegradation efficiency was found to diminish when the photocatalyst dose exceeded the optimum dose because of the growing opacity of the reaction mixture (suspension). Similarly, the reduced activity at lowed dose of photocatalyst is due to the insufficient number of active sites for photocatalysis.

Zinc nitrate hexahydrate was used as the precursor in the green synthesis of ZnO NPs. It is evident from Figure 9(a) (see Table 1 for composition) that the concentration of the precursor affected the efficiency of the as-synthesized ZnO NPs photocatalysts. It is also clear that 0.4 M concentration of zinc nitrate hexahydrate is the optimum concentration for the synthesis of efficient photocatalyst nanoparticles. As the concentration of zinc nitrate hexahydrate was increased from 0.3 to 0.4 M, there was no remarkable increase in the catalytic performance of the photocatalyst. Therefore, further concentration was not tested and 0.4 M concentration of zinc nitrate hexahydrate was used as the optimum concentration of the precursor solution for the green synthesis of ZnO NPs.

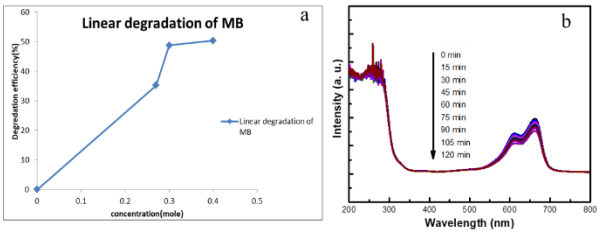

Figure 9: (a) Plot of molar concentration of ZnO NPs used vs degradation of MB and (b) Photodegradation of MB for 120 min of sunlight exposure with interval time of 15 min (blank test).

The effectiveness of the as-prepared nanoparticles was accessed through the comparison of their action with the blank test results. The corresponding information is presented in Figure 9 (b). It is evident from the figure that the photodegradation of MB in the absence of a photocatalyst is almost negligible. The slight degradation as indicated by the slight decline in the intensity of absorbance spectra is assigned to the self-degradation of MB due to self-sensitization.

Conclusion

Using an eco-friendly method, ZnO NPs were successfully synthesized employing *Citrus limon* (lemon) peel extract. Waste lemon peels were effectively used in the synthesis of ZnO NPs. The synthesized ZnO NPs displayed yellowish white mass in the reaction mixture which indicated the formation of ZnO NPs. Successful synthesis of the desired nanoparticles was affirmed through standard characterization techniques, namely, UV-vis spectroscopy, FE-SEM, HR-TEM, FT-IR and XRD analysis.

The UV-vis spectroscopic analysis showed the absorbance peak at 332 nm which indicated the formation of ZnO NPs. FE-SEM reveled irregular shape of nanoparticles without distinctly defined morphology. HR-TEM analysis revealed the microstructure and size of the prepared nanoparticles. X-ray diffraction confirmed the well crystalline form of the nanoparticles with hexagonal wurtzite structure. The average crystallite size as determined from the most intense XRD peak was 19 nm based on the Scherrer's formulae. The synthesized ZnO NPs synthesized by using optimum concentration of precursor, when used in optimum dose, resulted in notable degradation of 50.25% MB under solar light irradiation. It is anticipated that the as-synthesized photocatalyst will be a valued agent for the photocatalytic removal of persistent water pollutant dyes and assist in environmental detoxification.

References

1. Santoshi kumari, A. *et al*. 2015. Green synthesis, characterization and catalytic activity of palladium nanoparticles by xanthan gum. *Applied Nanoscience*. **5**:315-320.
2. Gur, T. *et al*. 2022. Green synthesis, characterization and bioactivity of biogenic zinc oxide nanoparticles. *Environmental Research.* **204**:111897.
3. Muhammad, W. *et al*. 2019. Optical, morphological and biological analysis of zinc oxide nanoparticles (ZnO NPs) using Papaver somniferum L. *Royal Society of Chemistry.* **9**(51):29541-29548.
4. Fakhari, S., Jamzad, M. and Kabiri Fard, H. 2019. Green synthesis of zinc oxide nanoparticles: a comparison. *Green Chemistry Letters and Reviews.* **12**(1):19-24.
5. Selim, Y. A. *et al*. 2020. Green synthesis of zinc oxide nanoparticles using aqueous extract of Deverra tortuosa and their cytotoxic activities. *Scientific Reports.* **10**(1):3445.
6. Vijayakumar, S. *et al*. 2018. Green synthesis of zinc oxide nanoparticles using Atalantia monophylla leaf extracts: Characterization and antimicrobial analysis. *Materials Science in Semiconductor Processing.* **82**:39-45.
7. Kaushik, M. *et al.* 2019. Investigations on the antimicrobial activity and wound healing potential of ZnO nanoparticles. *Applied Surface Science.* **479**:1169-1177.
8. Narain, R. (Ed.). 2020. Polymer science and nanotechnology: fundamentals and applications. *Elsevier*.
9. Brown, P. J. and Stevens, K. A. 2007. Nanofibers and nanotechnology in textiles. *CRC Press.*
10. Eaton, P. *et al*. 2017. A direct comparison of experimental methods to measure dimensions of synthetic nanoparticles. *Ultramicroscopy.* **182**:179-190.
11. Sadiq, H. *et al*. 2021. Green synthesis of ZnO nanoparticles from Syzygium Cumini leaves extract with robust photocatalysis applications. *Journal of Molecular Liquids.* **335**: 116567.
12. Din, M. I. *et al*. 2021. Fundamentals and photocatalysis of methylene blue dye using various nanocatalytic assemblies-a critical review. *Journal of Cleaner Production*. **298**:126567.
13. Sapkota, K. P. *et al.* 2021. Hierarchical nanocauliflower chemical assembly composed of copper oxide and single-walled carbon nanotubes for enhanced photocatalytic dye degradation. *Nanomaterials*. **11**(3): 696.
14. Haque, M. J. *et al*. 2020. Synthesis of ZnO nanoparticles by two different methods & comparison of their structural, antibacterial, photocatalytic and optical properties. *Nano Express.* **1**(1): 010007.
15. Jamdagni, P., Khatri, P., & Rana, J. S. 2018. Green synthesis of zinc oxide nanoparticles using flower extract of Nyctanthes arbor-tristis and their antifungal activity. *Journal of King Saud University-Science.* **30**(2): 168-175.
16. Ali, J., Das, B. and Saikia, T. R. I. D. E. E. P. 2017. Antimicrobial activity of lemon peel (*Citrus limon*) extract. *International Journal of Current Pharmaceutical Research*. **9**(4): 79-82.
17. Garibo, D. *et al*. 2020. Green synthesis of silver nanoparticles using Lysiloma acapulcensis exhibit high-antimicrobial activity. *Scientific Reports.* **10**(1): 12805.
18. Amer, M. and Awwad, A. 2020. Green synthesis of copper nanoparticles by Citrus limon fruits extract, characterization and antibacterial activity. *Chemistry International*. **7**(1): 1-8.
19. Awwad, A. M. *et al*. 2020. Green synthesis of zinc oxide nanoparticles (ZnO-NPs) using Ailanthus altissima fruit extracts and antibacterial activity. *Chemistry International*. **6**(3): 151-159.
20. Thang, P. Q. 2020. Green synthesis of copper nanoparticles using mandarin (citrus reticulata) peel extract and antifungal study: Recent advancement. *Current Strategies in Biotechnology and Bioresource Technology*. **126**.
21. Makni, M. *et al*. 2018. Citrus limon from Tunisia: Phytochemical and physicochemical properties and biological activities. *BioMed Research International.*
22. Moosavy, M. H. *et al*. 2017. Antioxidant and antimicrobial activities of essential oil of lemon (citrus limon) peel in vitro and in a food model. *Journal of Food Quality & Hazards Control.* **4**(2).
23. Sapkota, B., Chandra Prakash, & Varsha Jain. 2020. Preliminary Phytochemical screening and quantitative analysis of Citrus maxima (Brum) leaves extract. *International Journal of Research in Pharmacology and Pharmacotherapeutics.* **9**(1): 100-106.
24. Gupta, S. *et al*. 2021. Phytochemical analysis and antibacterial activity of different Citrus fruit peel. *International Journal of Pharmaceutical Sciences and Research.* **12**(11):5820-5826.
25. Chandraker, S. K. *et al*. 2020. Green synthesis of copper nanoparticles using leaf extract of Ageratum houstonianum Mill. and study of their photocatalytic and antibacterial activities. *Nano Express.* **1**(1): 010033.

26. Sapkota, K. P. *et al*. 2020. Enhanced visible-light photocatalysis of nanocomposites of copper oxide and single-walled carbon nanotubes for the degradation of methylene blue. *Catalysts.* **10**(297).
27. Shaikh, J. R. and Patil, M. 2020. Qualitative tests for preliminary phytochemical screening: An overview. *International Journal of Chemical Studies.* **8**(2): 603-608.
28. Epp, J. 2016. X-ray diffraction (XRD) techniques for materials characterization. In materials characterization using nondestructive evaluation (NDE) methods (pp. 81-124). Woodhead Publishing.
29. Al-Bedairy, M. A. and Alshamsi, H. A. H. 2018. Environmentally friendly preparation of zinc oxide, study catalytic performance of photodegradation by sunlight for rhodamine B dye. *Eurasian Journal of Analytical Chemistry*. **13(**6): 1-9.
30. Sapkota, K. P. *et al*. 2019. Solar-light-driven efficient ZnO–single-walled carbon nanotube photocatalyst for the degradation of a persistent water pollutant organic dye. *Catalysts.* **9**(6): 498.